The European Physical Journal E 11, 389-397 (2003)

Hydrodynamic instabilities in ferronematics

A.B. Ryskin, H. Pleiner,[a] H.W. Müller

Max Planck Institute for Polymer Research, POBox 3148, 55021 Mainz, Germany

Received 10 February 2003, in final form 3 July 2003

Abstract. In the hydrodynamic description of ferronematics there are various dynamic magnetic field effects, linear in the field strength, that are negligible in usual nematics, but can play a role in ferronematics. Here we investigate theoretically the influence of these new terms on the thermal convection (Rayleigh-Bénard) and the viscous fingering (Saffman-Taylor) instability in ferronematics in the presence of a strong magnetic field. We find that the instabilities are qualitatively changed due to the occurrence of a finite vorticity component – a feature that is known from simple liquids in the case of a superimposed mechanical rotation. We suggest to use the additional effects (cross-flow within convection rolls, oblique rolls, rotating fingers) for measuring the phenomenological coefficients involved.

PACS. 61.30.-v Liquid crystals – 75.50.Mm Magnetic liquids

1 Introduction

Nematic liquid crystals doped with single-domain ferro- or ferrimagnetic grains, usually denoted as ferronematics, are of great interest for potential applications but also under the scope of fundamental research. Starting with the pioneering work of Brochard and de Gennes [1] the idea came up to intensify the ponderomotive response of a nematic liquid crystal by doping it with a small amount of ferromagnetic particles. The strong orientational coupling between the magnetic grains and the surrounding nematogen matrix enhances the susceptibility of the director dynamics. Indeed, the magnetic-field strength necessary to affect the director is decreased by several orders of magnitude giving control over the orientational state of the liquid crystal by magnetic fields as weak as 100 Oe. This "superparamagnetic" response is the basis of many applications.

Considerable efforts were undertaken in the preparation of various colloidal dispersions of ferromagnetic particles in liquid crystals during recent years. Starting with the first report in 1970 of mixing magnetic grains with the nematic phase of MBBA [2], there was a number of reports on the production of mixtures of rod-like and disk-like nematics with magnetic grains [2–5]. In many systems investigated there were problems with chemical stability. Recently, however, the preparation of stable ferronematic systems has attracted increasing attention [6–14].

Apart from the strong response to external magnetic fields that shows up in a possible dependence of all susceptibilities and transport parameters on the square of the field strength, there are additional dynamic effects linear in the field strength [15]. In ordinary nematics those effects are always neglected, but in ferronematics with their strong sensitivity to magnetic fields there is the expectation that these effects are sufficiently enhanced. They can be described as linear-field-dependent additions to ordinary dynamic material tensors describing, for example, heat conduction, diffusion, electric conductivity, viscosity, flow alignment and relaxation of the director. Since a magnetic field is odd under time reversal symmetry, these new effects are reversible (non-dissipative) if the field-free part of the tensor describes a dissipative effect and vice versa. In isotropic systems a few of such effects are known (Hall and Righi-Leduc effect [16]).

In the following we address the question what are the consequences of these new linear-magnetic-field effects on hydrodynamic instabilities in ferronematics. In particular, we consider the well-known Rayleigh-Bénard and Saffman-Taylor instabilities and discuss how the general features of these instabilities are changed qualitatively due to the presence of the new contributions. The qualitatively new behavior can be used as a tool to measure the new field-dependent material parameters involved [15].

In this work we disregard the magnetization as an independent dynamic degree of freedom, but assume that it is relaxed to its equilibrium value and orientation on the time scale under consideration. This is in the spirit of the "rigid anchoring" approximation [1], implying that the relative orientation of the director $\mathbf{n}$ and the local magnetization $\mathbf{M}$ is fixed (being either parallel or perpendicular). However, with the synthesis of thermotropic ferronematics [17] it became evident that this approximation might not be generally applicable. The orientations of $\mathbf{n}$ and $\mathbf{M}$ were treated as separate degrees of freedom

[a] e-mail: pleiner@mpip-mainz.mpg.de

within the framework of a microscopic model [18] and in a hydrodynamic description [19]. We also assume that there is no spontaneous magnetization (true ferromagnetism), that means there is no remanent magnetization in the absence of an external field. Although such a ferromagnetic behavior is possible in principle [20], there is yet no experimental evidence for it.

2 Governing equations

As discussed in the Introduction we take the set of hydrodynamic equations given in [15] to describe ferronematics. Since we will use them to discuss Rayleigh-Bénard and Saffman-Taylor instabilities, we will apply the well-known Boussinesq approximation [21], i.e. take the flow as incompressible and all material parameters as well as the density as constant (ρ_0), except for the buoyancy force. We are then left with dynamic equations for the velocity field $\boldsymbol{v}$, the temperature T, and the director field $\boldsymbol{n}$

$$\rho_0(\frac{\partial v_i}{\partial t} + v_j\nabla_j v_i) = -\nabla_i p + \nu_{ijkl}\nabla_j\nabla_k v_l + \frac{1}{2}\tilde{\lambda}_{kji}\nabla_j h_k - \nabla_j(\Phi_{li}\nabla_i n_l) + \rho g_i \quad (1)$$

$$\mathrm{div}\boldsymbol{v} = 0 \quad (2)$$

$$\frac{C_V}{T}(\frac{\partial T}{\partial t} + v_i\nabla_i T) = \kappa_{ij}\nabla_i\nabla_j T \quad (3)$$

$$\frac{\partial n_i}{\partial t} + v_j\nabla_j n_i = -\frac{1}{2}\lambda_{ijk}\nabla_j v_k + (\gamma^{-1})_{ij}h_j \quad (4)$$

where on the r.h.s. of (3) dissipative nonlinearities (e.g. “viscous heating”) have been neglected. C_V is the specific heat at constant density, p is the pressure, $\boldsymbol{g}$ is the constant gravity force, while $\boldsymbol{h} \equiv \partial\epsilon/\partial\boldsymbol{n}$ (with ϵ the energy density) and $\Phi_{ij} \equiv \partial\epsilon/\partial\nabla_j n_i$ are the thermodynamic conjugates to homogeneous and inhomogeneous director reorientations [22]. The former describes the static response to external fields, while the latter contains the Frank rotational elasticity. The induced magnetization is assumed to be fixed by the external field and is not a dynamic variable. The concentration of magnetic particles is very low and we neglect the Kelvin force.

The material tensors, in linear order of the external magnetic field, are the sum of a constant part and a linear one

$$\nu_{ijkl} = \nu^D_{ijkl} + \nu^R_{ijkl}(H), \quad (5)$$

$$\kappa_{ij} = \kappa^D_{ij} + \kappa^R_{ij}(H), \quad (6)$$

$$\lambda_{ijk} = \lambda^R_{ijk} + \lambda^D_{ijk}(H), \quad (7)$$

$$\tilde{\lambda}_{kji} = \lambda^R_{kji} - \lambda^D_{kji}(H), \quad (8)$$

$$(\gamma^{-1})_{ij} = (\gamma^{-1})^D_{ij} + (\gamma^{-1})^R_{ij}(H), \quad (9)$$

and describe viscosity, heat conduction, flow alignment and director relaxation, respectively. Their general form is listed in [15, 22] and will be given below, as far as needed. Note that the thermodynamic nature of the different contributions changes from dissipative (superscript D) to reversible (superscript R), or vice versa, since the magnetic field transforms odd under time reversal. Thus, the field-free contributions to the dynamics always have a different time reversal behavior compared to those linear in the field, which in turn gives rise to the different thermodynamic properties. This is reflected also in the different symmetry properties (Onsager relations), i.e. symmetric in the dissipative parts ($\kappa^D_{ij} = \kappa^D_{ji}$, $\nu^D_{ijkl} = \nu^D_{klij}$, $(\gamma^{-1})^D_{ij} = (\gamma^{-1})^D_{ji}$) and antisymmetric in the reversible parts ($\kappa^R_{ij}(H) = -\kappa^R_{ji}(H)$, $\nu^R_{ijkl}(H) = -\nu^R_{klij}(H)$, $(\gamma^{-1})^R_{ij}(H) = -(\gamma^{-1})^R_{ji}(H)$) and in the difference between λ_{ijk} and $\tilde{\lambda}_{ijk}$ in (1) and (4).

It is the purpose of this work to investigate the influence of the linear field contributions to the transport tensors (and mainly that of $\nu^R_{ijkl}(H)$) on various instabilities. We do this in the approximation of very strong fields, since in that limit there is the best chance that the proposed new effects are observable. Specifically, we assume that the director relaxes to its equilibrium orientation, defined by the external field, on a time scale much smaller than that of the other relevant variables. In that case $\partial n_i/\partial t = 0$ and the director is clamped. The larger the field the better is this approximation. For ordinary nematics (5CB) the field necessary to clamp the director is about 1 kGauss [23] and probably smaller for ferronematics, since their response to magnetic fields generally is stronger.

This approximation is similar in spirit to the incompressibility assumption, where the density variations are supposed to live on a much shorter time scale than the other relevant variables (i.e. the relevant velocities are much smaller than the sound velocity). When density variations are not a dynamic variable, its conjugate, the chemical potential or the pressure is no longer determined thermodynamically. The pressure is used to guarantee the incompressibility for all times, i.e. $\partial\mathrm{div}\boldsymbol{v}/\partial t = 0$, which leads to a condition on $\boldsymbol{\nabla}^2 p$ in eq.(1). Eliminating the director as a dynamic variable has the consequence that its conjugate, $\boldsymbol{h}$ is not defined, but rather functions to guarantee $\boldsymbol{n} = const.$ for all times, thus reducing eq.(4) to

$$h_i = \gamma_{ji}\frac{1}{2}\lambda_{jkl}\nabla_k v_l \quad (10)$$

where $\gamma_{pm}(\gamma^{-1})_{mq} \equiv \delta^{tr}_{pq}$. Substituting this in (1) we regain for this equation a form familiar from simple liquids

$$\rho_0(\frac{\partial v_i}{\partial t} + v_j\nabla_j v_i) = -\nabla_i p + \nu^{eff}_{ijkl}\nabla_j\nabla_k v_l + \rho g_i \quad (11)$$

but with an effective viscosity tensor

$$\nu^{eff}_{ijkl} = \nu_{ijkl} + \frac{1}{4}\tilde{\lambda}_{pji}\gamma_{pm}\lambda_{mkl} \quad (12)$$

Since we are concentrating on linear field effects eq.(12) can be simplified

$$\nu^{eff}_{ijkl} = \nu^D_{ijkl} + \nu^R_{ijkl}(H) + \frac{1}{4}\lambda^R_{pji}\gamma^D_{pm}\lambda^R_{mkl} + \frac{1}{4}\gamma^D_{pm}\left(\lambda^R_{pji}\lambda^D_{mkl}(H) - \lambda^D_{pji}(H)\lambda^R_{mkl}\right) + \frac{1}{4}\lambda^R_{pji}\gamma^R_{pm}(H)\lambda^R_{mkl} \quad (13)$$

where the γ_{ij} tensors are given by

$$\gamma_{ij}^D = \gamma_1 \delta_{ij}^{tr} \tag{14}$$

$$\gamma_{ij}^R = -\frac{\gamma_1^2}{\gamma_1^R}\epsilon_{ijk} n_k n_l H_l - \frac{\gamma_1^2}{\gamma_2^R}\left(\epsilon_{ijp} + \epsilon_{ipk} n_k n_j - \epsilon_{jpk} n_k n_i\right) H_p \tag{15}$$

Here the coefficients γ_1^R, γ_2^R are those introduced in [15].

The explicit forms of this effective viscosity tensor will be discussed for the two cases $\boldsymbol{n} \parallel \boldsymbol{H}$ and $\boldsymbol{n} \perp \boldsymbol{H}$ below.

The heat conduction equation (3) also contains a new linear field effect through $\kappa_{ij}^R(H)$ (6). However, in this case the bulk effect vanishes, since both, $\nabla_i \kappa_{ij}^R = 0$, because of $\boldsymbol{n} = const$ and the Boussinesq approximation, and $\kappa_{ij}^R \nabla_i \nabla_j T = 0$, because of $\kappa_{ij}^R(H) = -\kappa_{ji}^R(H)$. Thus, this linear field effect will only appear in boundary conditions, if they are formulated in terms of the heat flux. We will not consider such boundary conditions in what follows.

In the next section we will investigate how the new terms (13) manifest themselves in the thermo-gravitational instability.

3 Rayleigh-Bénard instability

3.1 The case when $\boldsymbol{n} \parallel \boldsymbol{H}$

We consider an infinitely extended layer of ferronematic liquid crystal bounded by two rigid parallel plates at distance h. The temperature of the plates is kept fixed at T_1 and $T_0 > T_1$ (Fig. 1). An external magnetic field is imposed in z-direction ($\hat{\boldsymbol{e}}_z$) and the gravitational force works in $-z$-direction ($\boldsymbol{g} = -g\hat{\boldsymbol{e}}_z$). In the case of a positive magnetic susceptibility anisotropy $\chi_a > 0$ the director tends to align along the magnetic field. Homeotropic boundary conditions for the director are helpful. We assume the magnetic field to be strong enough that the director is clamped

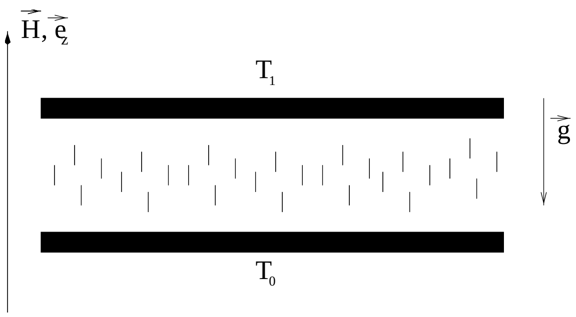

Fig. 1. Sketch of the setup in the parallel case. For details see text.

$$\boldsymbol{n} = \frac{\boldsymbol{H}}{|\boldsymbol{H}|} \tag{16}$$

and does not have an independent dynamics. The magnetic field in the sample is always taken as static and uniform, and equal to the value of external field (eventually corrected by some demagnetization factor). Thus the system is described by the effective Navier-Stokes equation (11), incompressibility (2) and heat conduction (3).

The trivial heat conduction state, without any flow and a linear temperature profile is always a solution:

$$\boldsymbol{v} = 0 \tag{17}$$

$$T(z) = -\frac{T_0 - T_1}{h} z + T_0 \tag{18}$$

$$\rho(z) = \rho_0 \left(1 + \alpha_p \frac{T_0 - T_1}{h} z\right) \tag{19}$$

with $\alpha_p = -(1/\rho)(\partial\rho/\partial T)_p$ the thermal expansion coefficient.

However, this solution is stable for small temperature differences only and is subject to the Rayleigh-Bénard instability, when the temperature difference exceeds some threshold value. To find this threshold value in terms of the material parameters involved, we study the stability of small perturbations of the ground state (17-19) by linearizing (2,3,11) around the conduction state

$$\partial_t v_i = -\frac{\nabla_i p'}{\rho_0} + \mu_{ijkl}^{eff} \nabla_j \nabla_k v_l - g\,\alpha_p\,\theta \delta_{i,z} \tag{20}$$

$$\partial_t \theta - w = k_{ij} \nabla_i \nabla_j \theta \tag{21}$$

$$div \boldsymbol{v} = 0 \tag{22}$$

Here $\boldsymbol{v}$ is the velocity field ($w = v_z$), θ is the deviation of the temperature field from the linear profile (18) and p' the pressure perturbation. The temperature conduction tensor $k_{ij} = k_\perp (\delta_{ij} - n_i n_j) + k_\parallel n_i n_j$ is related to the heat conduction tensor $\kappa_{ij} = (C_V/T) k_{ij}$ and the effective kinematic viscous tensor $\mu_{ijkl}^{eff} = (1/\rho_0)\nu_{ijkl}^{eff}$ is connected to the effective dynamic viscosity ν_{ijkl}^{eff} (12).

The complicated tensors (5-9) that enter μ_{ijkl}^{eff} can be simplified in the special case $\boldsymbol{n} \parallel \boldsymbol{H}$ considered here with the result

$$\begin{aligned}
\rho_0\, \mu_{ijkl}^{eff} = {} & \nu_2 \left(\delta_{jl}\delta_{ik} + \delta_{il}\delta_{jk}\right) \\
& + 2(\nu_1 + \nu_2 - 2\nu_3 + \tfrac{1}{2}\gamma_1 \lambda^2)\, n_i n_j n_k n_l \\
& + (\nu_3 - \nu_2)(n_j n_l \delta_{ik} + n_j n_k \delta_{il} + n_i n_k \delta_{jl} + n_i n_l \delta_{jk}) \\
& + \tfrac{1}{4}\gamma_1 \left((\lambda - 1)^2 \delta_{jk} n_i n_l + (\lambda + 1)^2 \delta_{il} n_j n_k\right) \\
& + \tfrac{1}{4}\gamma_1 (\lambda^2 - 1)(\delta_{jl} n_i n_k + \delta_{ik} n_j n_l) \\
& + H(\bar{\nu}_1^R \varepsilon_{ikp} n_j n_l n_p + \bar{\nu}_2^R \varepsilon_{ilp} n_j n_k n_p) \\
& \quad + \bar{\nu}_3^R \varepsilon_{jlp} n_i n_k n_p + \bar{\nu}_4^R \varepsilon_{jkp} n_i n_l n_p) \\
& + \bar{\bar{\nu}}^R H(\varepsilon_{ikp}\delta_{jl} n_p + \varepsilon_{ilp}\delta_{jk} n_p + \varepsilon_{jkp}\delta_{il} n_p + \varepsilon_{jlp}\delta_{ik} n_p)
\end{aligned} \tag{23}$$

where for the field-free viscosities ($\nu_{1,2,3}$) the Harvard notation [24] is used, λ is the flow alignment parameter [25], and γ_1 the rotational viscosity [26]. The abbreviations $\bar{\nu}_\alpha^R$ and $\bar{\bar{\nu}}^R$ that are related to the new field-dependent effects are listed in the Appendix (A.1).

We non-dimensionalize equations (20-22) by taking the layer thickness h as length scale, $h^2/k_\perp$ as time scale and the difference $T_0 - T_1$ as temperature scale. With the usual procedure [21] of taking $(curl\ curl)_z$ as well as $curl_z$ of the eq.(20) we get for w, $\xi \equiv (curl\boldsymbol{v})_z$ and θ

$$\frac{1}{Pr}\partial_t\left(\Delta_2+\partial_z^2\right)w = \left(a\,\partial_z^4 + b\Delta_2\partial_z^2 + c\Delta_2^2\right)w + Ra\Delta_2\theta$$
$$+\overline{H}_1\left(e\Delta_2-\partial_z^2\right)\partial_z\xi - \overline{H}_2\left(\Delta_2+\partial_z^2\right)\partial_z\xi \qquad (24)$$

$$\frac{1}{Pr}\partial_t\xi = \left(\Delta_2 + a\,\partial_z^2\right)\xi - \overline{H}_1\left(d\Delta_2 - \partial_z^2\right)\partial_z w$$
$$+\overline{H}_2\left(\Delta_2+\partial_z^2\right)\partial_z w \qquad (25)$$

$$\partial_t\theta - w = \partial_z^2\theta + \alpha\Delta_2\theta \qquad (26)$$

with the 2-dimensional Laplace operator $\Delta_2 = (\partial_x^2 + \partial_y^2)$. The material dependent coefficients are $a = (\nu_3 + \frac{1}{4}\gamma(1+\lambda)^2)/\nu_2$, $b = (2\nu_1 + 2\nu_2 - 2\nu_3 + \frac{\gamma_1}{2}(\lambda^2+1))/\nu_2$, $c = (\nu_3 + \frac{1}{4}\gamma(1-\lambda)^2)/\nu_2$, $d = \bar{\nu}_1^R/\bar{\nu}_2^R$, $e = \bar{\nu}_3^R/\bar{\nu}_2^R$, and $\alpha = \kappa_\parallel/\kappa\perp$, with Ra the Rayleigh number $Ra = gh^3\alpha_p(T_0 - T_1)/(\nu_2 k_\perp)$ and Pr the Prandtl number $Pr = \nu_2/k_\perp$. The magnetic field enters in the non-dimensional form $\overline{H}_1 = \bar{\nu}_2^R H/\nu_2$ and $\overline{H}_2 = \bar{\bar{\nu}}^R H/\nu_2$.

One can see that in addition to the degrees of freedom that are necessary to describe the Rayleigh-Bénard instability in usual nematics, there is also ξ, the z - component of the vorticity. This situation is similar to the case of the thermal instability in a rotating layer of simple liquids [21]. In both cases the time reversal symmetry is broken by the external (flow or magnetic) field. In our geometry we expect a roll pattern due to the spatial up-down or mid-plane symmetry that is still present. In such a pattern the z-component of the vorticity is manifest as a crossflow in the $x-y$ plane as shown in Fig. 2. Measuring this component of the velocity can serve as a direct indication of the presence of the new field-dependent terms in the viscosity tensor. Although ferrofluids are rather dark and flow is difficult to view directly, reflecting tracer particles may be used.

We have determined the threshold of the stationary instability taking for example the material parameters of MBBA liquid crystals. Assuming non-slip boundary condition we use the method suggested in [27]. On Fig. 3 one can see the threshold as a function of the non-dimensional magnetic field $\overline{H} = \overline{H}_1 + \overline{H}_2 = H(\nu_4^R + \nu_5^R + \nu_7^R + 3\nu_8^R)/\nu_2$ for the case $\bar{\nu}_1^R = \bar{\nu}_2^R = \bar{\nu}_3^R = \bar{\nu}_4^R = \bar{\bar{\nu}}^R$ (this additional assumption is made for representative reasons only). For low fields the threshold is a quadratic function of the magnetic field, which is to be expected, since the Rayleigh number is a scalar while the magnetic field is a vector. This quadratic field dependence is not specific for the new contributions in the viscosity tensor, since any (trivial) H^2-dependence of material parameters would produce such an effect. The $\overline{H}$ effect on Ra_c is rather small. In order to get a 3% increase, $\overline{H}$ has to be about 0.5 requiring the field H and the typical ν_α^R to be so large that $H\nu_\alpha^R$ is about one order of magnitude smaller than the ordinary shear viscosity ν_2.

The high value of the threshold without field is due to our assumption of quenched director orientation, which leads to the presence of the additional terms $\lambda_{pji}^R\gamma_{pm}^D\lambda_{mkl}^R$ in the viscosity tensor (13). For very high fields, which are probably beyond experimental reach, $Ra_c \sim \overline{H}^{4/3}$, asymptotically. Comparing with the case of a Rayleigh-Bénard experiment under rotation in simple fluids [21], where an oscillatory instability is possible for very low Prandtl numbers, we expect the instability to be always stationary here, since $Pr \gg 1$ in nematics. In the rotation case, the stationary rolls are known to be subject to the Küppers-Lortz secondary instability into a non-stationary state at even higher Rayleigh number $Ra > Ra_c$ [28], and this behavior can be expected here in the ferronematic case, too.

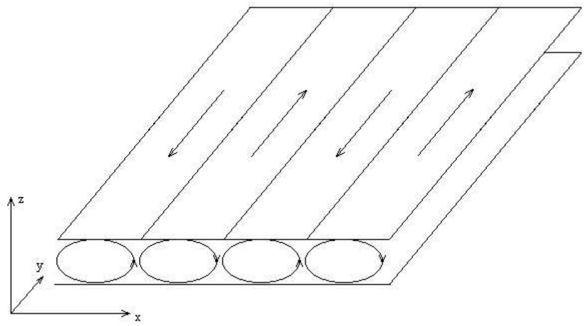

Fig. 2. The effect of the new field-dependent terms in the effective viscosity tensor on the convection roll pattern. The flow due to the non-zero vorticity component is shown by arrows on the top; at the bottom the arrows are in opposite direction. The orientation of the rolls is chosen to be the y-direction, arbitrarily.

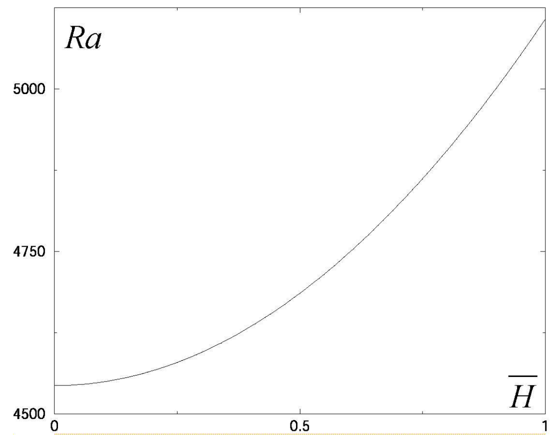

Fig. 3. The critical Rayleigh number Ra_c as a function of the magnetic field $\overline{H}$ (parallel case).

3.2 The case when $\boldsymbol{n} \perp \boldsymbol{H}$

When the magnetic susceptibility anisotropy is negative $\chi_a < 0$, the director field tends to be perpendicular to the magnetic field. This is the typical case for lyotropic systems. Here, in principle also concentration and mixture effects have to be taken into account. They are known to play a considerable role in thermal instabilities in isotropic ferrofluids (cf. e.g. [29]), but their inclusion here is way beyond the scope of the present work.

To consider the influence of the new magnetic field dependent terms we consider the geometry shown in Fig. 4. As in the previous case we have an infinite layer of ferronematics subject to a temperature gradient across the layer. An external magnetic field is imposed along the temperature gradient (z-direction,) while the nematic director is oriented perpendicular (y-direction). We assume that also a strong electric field is applied, in order to clamp the director in its equilibrium orientation. Thus, like in the preceding section, director reorientations are neglected. In this case the equations describing linear stability analysis are again given by Eqs.(20-22), where the effective viscosity tensor (13) now takes the form (A.2) given in the Appendix.

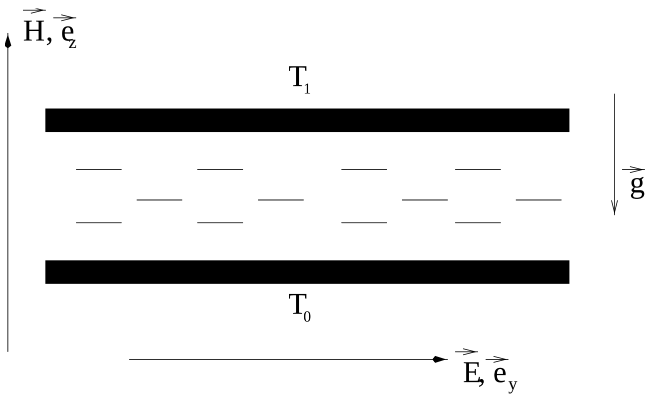

Fig. 4. Sketch of the setup in the perpendicular case. For details see text.

We also assume that the magnetic field dependent contributions come only from the viscosity tensor, i.e. we neglect all λ_α^D in (A.3). Otherwise we need to explore a parameter space of very high dimension. This is not reasonable at present, since those parameters are unknown and we are interested in qualitative effects only. In this case the magnetic field enters the equations through two material dependent dimensionless coefficients

$$\begin{aligned} \overline{H}_1 &= (\nu_2^R - \nu_7^R + \nu_8^R)H/\nu_2 \\ \overline{H}_2 &= (\nu_1^R + \nu_2^R - 2\nu_5^R - \nu_7^R - 3\nu_8^R)H/\nu_2 \end{aligned} \tag{27}$$

which contain combinations of the ν_α^R ($\alpha = 1...8$) introduced in [15]. If no magnetic field is present, the behavior of the system is that of a pure simple liquid and the convection sets in at $Ra_c = 1708$, because the heat focusing effect of nematics [30] is suppressed by clamping the director. Comparing with the case $\boldsymbol{n} \parallel \boldsymbol{H}$ the clamped nematic degree of freedom now is inoperative with respect to the onset of the instability, but sets the direction of the rolls.

If we switch on the external magnetic field, the new dynamic field-dependent terms come into play and the instability picture changes considerably. To study this problem in more detail we use a three dimensional analysis introduced in [31]. The velocity field is represented by two scalar potentials f and g

$$\boldsymbol{v} = \begin{pmatrix} \partial_x \partial_z f + \partial_y g \\ \partial_y \partial_z f - \partial_x g \\ -\partial_x \partial_x f - \partial_y \partial_y f \end{pmatrix} \tag{28}$$

Due to the homogeneity in the lateral directions we can take all fields to be of the form $\{f, g, \theta\} = \{f(z), g(z), \theta(z)\} exp\{i\boldsymbol{kr} + i\omega t\}$, where $\boldsymbol{k}$ is a two-dimensional wave vector in the $x - y$ plane. Substituting (28) into the linearized equations (20-22) and taking $curl_z$ as well as $(curl\, curl)_z$ of (20) we get the linear system of equations

$$\hat{L}(Ra, k_x, k_y, \omega, \overline{H}_1, \overline{H}_2) \begin{pmatrix} f \\ g \\ \theta \end{pmatrix} = 0 \tag{29}$$

where $\hat{L}$ is a linear differential operator of eighth order with respect to z. The explicit form of Eqs.(29) is presented in (A.4-A.6) in the Appendix. No-slip boundary conditions translate into

$$\begin{aligned} f(0) = f(1) = f'(0) = f'(1) = 0 \\ g(0) = g(1) = 0 \\ \theta(0) = \theta(1) = 0 \end{aligned} \tag{30}$$

To find the threshold of a stationary instability we take $\omega = 0$. At any given values of k_x, k_y, $\overline{H}_1$,and $\overline{H}_2$ the problem is to find the value Ra such that the boundary value problem (29-30) has a nontrivial solution. The function $Ra(k_x, k_y)$ is then minimized to find the threshold Ra_c for the given values of $\overline{H}_1$ and $\overline{H}_2$.

The solution of this problem was accomplished using the shooting method presented in Ref. [27]. Here the system of linear differential equations is solved using a matrix representation of the solution. The parameters were taken as those for MBBA liquid crystals. In order to simplify the presentations of the results we take $\overline{H}_2 = 0$ ($\overline{H}_1 = \overline{H}$). This additional assumption does not change the qualitative picture of the instability, nor does it affect the limiting cases $H = 0$ and $H \to \infty$. In the case of zero magnetic field the minimum of the function $Ra(k_x, k_y)$ is on the line $k_y = 0$, which corresponds to rolls aligned along the nematic director. The critical Rayleigh number is then $Ra_c = 1708$ as expected [30]. Increasing slightly the strength of the magnetic field leads to an increase in Ra_c, but k_y is still zero. When the value of $\overline{H}$ exceeds some critical value $\overline{H}_\ell$ the minimum of the function $Ra(k_x, k_y)$ shifts to a finite $k_y \neq 0$. On Fig. 5 the dependence of k_x and k_y on $\overline{H}$ is presented. The appearance of a finite k_y above $\overline{H}_\ell$ is accompanied by a strong drop of k_x. The critical $\overline{H}_\ell$ already corresponds to a rather large field H, for

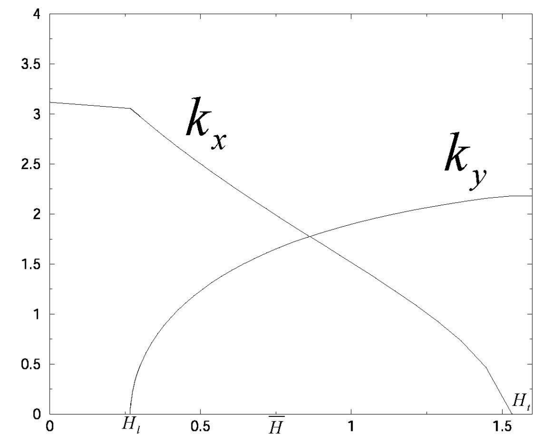

Fig. 5. The wave vector components k_x and k_y corresponding to the minimum of the function $Ra_c(k_x, k_y)$ as a function of the magnetic field $\overline{H}$.

which the product with a typical ν_α^R, $H\nu_\alpha^R$, is almost of the order of the shear viscosity ν_2.

When the magnetic field is increased further above $\overline{H}_t$, finally $k_x = 0$. The minimum of $Ra(k_x, k_y)$ is then along the line $k_x = 0$ and the rolls are aligned perpendicular to the director. Any further increase of $\overline{H}$ does not change the position of the rolls, nor the value of the critical Rayleigh number. The threshold value as a function of the magnetic field is presented in Fig. 6.

Analyzing these results we can predict the corresponding flow patterns. First, when $\overline{H} < \overline{H}_\ell$ the convective rolls are aligned along the electric field. When the magnetic field exceeds this lower critical value $\overline{H}_\ell$, the rolls get oblique with respect to the electric field and the angle between the rolls and the electric field increases with increasing magnetic field. At the point when the magnetic field reaches the upper critical value H_t, the rolls are perpendicular to the electric field and stay so for any higher field. Note that the director is always parallel to the electric field (and perpendicular the external magnetic field). Thus, in the intermediate magnetic field regime the director is oblique to the roll orientation, while in the high field regime it is perpendicular. It is possible that this high field regime cannot be reached in actual experiments.

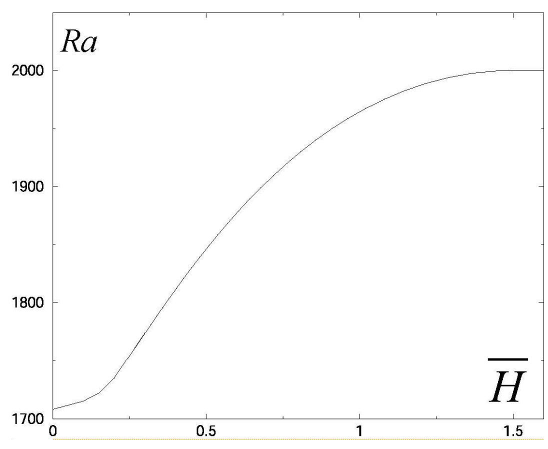

Fig. 6. The critical Rayleigh number Ra_c as a function of the magnetic field $\overline{H}$ (perpendicular case).

We have looked numerically for an oscillatory instability, but did not find any. Since this search could be done for a limited parameter range only, this is no proof for a general absence of an oscillatory instability. In principle, the set of equations (29,30) can support non-trivial solutions at a finite frequency $\omega \neq 0$, since it is not self-adjoint.

4 Saffman-Taylor instability

Another useful tool to study the new linear field dependent contributions in the effective viscosity tensor is flow in a Hele-Shaw cell. When a viscous fluid is displaced by a less viscous one in the narrow space of a Hele-Shaw cell the Saffman-Taylor instability arises [32]. We consider a radial Hele-Shaw cell (Fig. 7), which consists of two parallel transparent plates at a distance d. The gap between them is filled with a high viscosity fluid, in our case a ferronematic. The low viscosity one (usually air) is injected through an inlet at the center of the upper plate. A magnetic field is imposed perpendicular to the plates (in z-direction) strong enough for the nematic director to be clamped. Here we again assume that the magnetic susceptibility anisotropy is positive and the director field is aligned parallel to the external field.

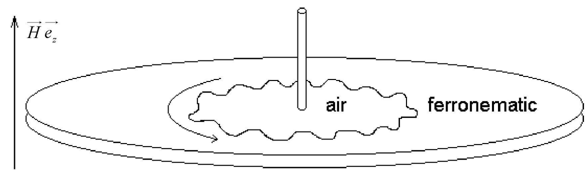

Fig. 7. The setup of a radial Hele-Shaw cell. For a ferronematic the external magnetic field leads to the rotation of the fingers shown by the arrow.

The description of the fluid motion far from the interface follows the usual lines [33]. Neglecting the inertia terms in the Navier-Stokes equation (11) we have

$$\partial_i p = \rho_0 \, \mu_{ijkl}^{eff} \, \partial_j \partial_k \, v_l \qquad (31)$$

where $\rho_0 \mu_{ijkl}^{eff}$ is given by (23) and the pressure gradient is constant along the radial directions. Since the gap d is small, we can neglect all derivatives of the velocity except those along the z-direction. Integrating (31) twice and taking the mean with respect to z-direction we get a linear relation between the mean velocity and the pressure gradient

$$v_i = -\frac{d^2}{12(A^2 + B^2)}(A\delta_{ij} - B\epsilon_{ijz})\partial_j p \qquad (32)$$

$$\text{with} \quad A = \nu_3 + \tfrac{1}{4}\gamma(1-\lambda)^2$$
$$B = H(\bar{\nu}_2^R + \bar{\bar{\nu}}^R)$$

where $\bar{\nu}_2^R$ and $\bar{\bar{\nu}}^R$ are given in Eq.(A.1). In cylindrical coordinates (r, θ, z) there is – apart from the usual radial component of the mean velocity v_r parallel to the pressure gradient – now also an azimuthal mean velocity component v_θ perpendicular to the pressure gradient, due to the new linear field terms in the effective viscosity tensor.

We will now consider how this azimuthal component of the velocity changes the picture of the Saffman-Taylor instability in the radial Hele-Shaw cell. Without perturbations the interface between the ferronematic liquid and the air is a circle with radius $R(t)$ (measured from the point of injection) that increases in time according to the radial velocity (normal to the interface) $v_n = v_r$. The tangential velocity, can be related to the normal one

$$v_T = v_\theta = \frac{B}{A} v_n \tag{33}$$

We investigate the linear stability of this interface with respect to azimuthal shape distortions "fingers") by assuming the interface to be located at $r(\theta, t) = R(t) + \zeta(\theta, t)$, with small perturbations $\zeta(\theta, t)$. The time evolution of these perturbations is related to perturbations, δv_n, in the normal velocity by the linearized kinematic condition

$$\partial_t \zeta + v_T \nabla_T \zeta = \delta v_n \tag{34}$$

taken at the undistorted interface $R(t)$. Here the tangential velocity v_T enters, since the distorted interface is no longer circular. Since the function $\zeta(\theta, t)$ has to be periodic in θ in order to have a well-defined interface, we can decompose it into discrete modes

$$\zeta(\theta, t) = \sum_{m=1}^{m=\infty} \zeta_m(t) \cos(m\theta + \phi_m(t)) \tag{35}$$

and make the linear stability analysis for each Fourier mode separately. We have allowed for a (still unknown) phase $\phi_m(t)$ for each mode. For the perturbations of the normal velocity we can write in linear approximation

$$\delta v_n = \sum_{m=1}^{m=\infty} \zeta_m(t) \widehat{\mu_m}(\theta, t) \cos(m\theta + \phi(t)) \tag{36}$$

where $\widehat{\mu_m}(\theta, t)$ is an operator with respect to θ. The actual form of this operator depends on the details of the boundary conditions [34]. We will assume for simplicity that $\widehat{\mu_m}(\theta, t)$ is independent of v_T. This is justified as long as the interface forces are not drasticaly altered by the magnetic field. Then it has the usual form

$$\widehat{\mu_m}(\theta, t) = a(R(t), m) + b(R(t), m) \frac{\partial^2}{\partial \theta^2} \tag{37}$$

where the explicit expressions for the functions $a(m)$ and $b(m)$ are rather involved and are the subject of special investigations (see for example [35]) due to the non-trivial physical mechanism involving the capillary force. However, since we are interested in the qualitatively new effects due to the finite tangential velocity v_T, the special form of $a(m)$ and $b(m)$ is unimportant here.

Substituting (35) and (36) into (34) and taking into account (37) we get for ζ_m and ϕ_m

$$\dot{\zeta}_m(t) = -\mu_m(t)\, \zeta_m(t) \tag{38}$$

$$\dot{\phi}_m = -m \frac{v_T}{R(t)} \tag{39}$$

where v_T is taken at $R(t)$. Here $\mu_m \equiv -a(R(t), m) + m^2\, b(R(t), m) = 0$ defines implicitly the most unstable mode. This pattern of fingers is rotating with angular velocity $m v_T / R(t)$ due to the time evolution of the phase $\phi(t)$. Within our assumptions the phase evolution (39) is completely decoupled from that of the amplitude and the details of $a(m)$ and $b(m)$ are unimportant. The amplitude equation (38) is independent of the new viscosity contributions and all previous investigations of the Saffman-Taylor instabilities for simple nematic liquid crystal (see for example [32]) are valid in this respect also for ferronematics. But in addition to the amplitude amplification there is the rotation of the growing fingers with angular velocity

$$\dot{\phi}_m = -\frac{mQ}{2\pi R(t)^2 d} \frac{B}{A} \tag{40}$$

where we have used eq. (33) to express v_T by v_n. The flow rate of the injected air, Q, is related to the normal velocity of the interface by $Q = 2\pi d\, R(t)\, v_n$.

5 Conclusion

We have discussed typical hydrodynamic instabilities in ferronematics under the aspect of qualitatively new effects due to the linear magnetic-field contributions to the dynamics of those materials. In Rayleigh-Bénard instabilities with the temperature gradient adverse to gravity we find, in addition to convection flow in the form of one-dimensional rolls, a vorticity flow. As a consequence, in the homeotropic case (the director parallel to the field) the streamlines are oblique to the roll cross-section, while in the planar case (the director perpendicular to the magnetic, but parallel to an electric field) the rolls themselves are tilted with respect to the director depending on the magnetic field strength. In the Saffman-Taylor viscous fingering instability of a growing interface between fluids of different density, the new linear magnetic-field contributions lead to a rotation of the finger structure. All these effects exist in principle in any nematic liquid crystal, since they are connected to the nematic degree of freedom, only, and not to the magnetization as an independent variable. In ordinary nematics, however, the interaction with magnetic fields is very weak and those effects have never been observed. In ferronematics, where the static response to magnetic fields is known to be enhanced by several orders of magnitude, one can expect that the influence of the magnetic field on the dynamics is also increased and strong enough to make the effects described here measurable.

Appendix A.

Appendix A.1. The form of the coefficients $\bar{\nu}_\alpha^R$ and $\bar{\bar{\nu}}^R$

Here we express the abbreviations $\bar{\nu}_\alpha^R$ and $\bar{\bar{\nu}}^R$ introduced in (23) by the coefficients introduced in [15]:

$$\begin{aligned}
\bar{\nu}_1^R &= \nu_4^R + \nu_5^R + 2\nu_8^R - \frac{\gamma_1^2}{4}\left(\frac{1}{\gamma_1^R} + \frac{1}{\gamma_2^R}\right)(\lambda^2 - 1) \\
&\quad -\frac{\gamma_1}{2}\left(\lambda_1^D + \lambda_3^D + \lambda_4^D\right)\lambda \\
\bar{\nu}_2^R &= \nu_4^R + \nu_5^R + 2\nu_8^R - \frac{\gamma_1^2}{4}\left(\frac{1}{\gamma_1^R} + \frac{1}{\gamma_2^R}\right)(\lambda + 1)^2 \\
&\quad -\frac{\gamma_1}{2}\left(\lambda_1^D + \lambda_3^D + \lambda_4^D\right)(\lambda + 1) \\
\bar{\nu}_3^R &= \bar{\nu}_1^R \\
\bar{\nu}_4^R &= \nu_4^R + \nu_5^R + 2\nu_8^R - \frac{\gamma_1^2}{4}\left(\frac{1}{\gamma_1^R} + \frac{1}{\gamma_2^R}\right)(\lambda - 1)^2 \\
&\quad -\frac{\gamma_1}{2}\left(\lambda_1^D + \lambda_3^D + \lambda_4^D\right)(\lambda - 1) \\
\bar{\bar{\nu}}^R &= \nu_7^R + \nu_6^R
\end{aligned} \tag{A.1}$$

Appendix A.2. The effective viscosity tensor in the case when $\boldsymbol{n} \perp \boldsymbol{H}$

With $\boldsymbol{H} = H\boldsymbol{e}_z$ and $n_i = \delta_{iy}$ we get

$$\begin{aligned}
\rho_0\, \mu_{ijkl}^{eff} &= \nu_2\left(\delta_{jl}\delta_{ik} + \delta_{il}\delta_{jk}\right) \\
&+2(\nu_1 + \nu_2 - 2\nu_3 + \tfrac{1}{2}\gamma_1\lambda^2)\, n_i n_j n_k n_l \\
&+(\nu_3 - \nu_2)(n_j n_l \delta_{ik} + n_j n_k \delta_{il} + n_i n_k \delta_{jl} + n_i n_l \delta_{jk}) \\
&+\tfrac{1}{4}\gamma_1\left((\lambda - 1)^2 \delta_{jk} n_i n_l + (\lambda + 1)^2 \delta_{il} n_j n_k\right. \\
&\left.+(\lambda^2 - 1)(\delta_{jl} n_i n_k + \delta_{ik} n_j n_l)\right) \\
&-H\,(\hat{\nu}_{1a}^R \delta_{ix} n_j n_k n_l + \hat{\nu}_{1b}^R \delta_{jx} n_i n_k n_l - \hat{\nu}_{1b}^R \delta_{kx} n_j n_i n_l \\
&-\hat{\nu}_{1a}^R \delta_{lx} n_j n_k n_i + \hat{\nu}_{2a}^R \delta_{jx} n_l \delta_{ik} - \hat{\nu}_{2b}^R \delta_{lx} n_j \delta_{ik} \\
&+\hat{\nu}_{2b}^R \delta_{jx} n_k \delta_{il} - \hat{\nu}_{2b}^R \delta_{kx} n_j \delta_{il} + \hat{\nu}_{2b}^R \delta_{ix} n_k \delta_{jl} \\
&-\hat{\nu}_{2a}^R \delta_{kx} n_i \delta_{jl} + \hat{\nu}_{2a}^R \delta_{ix} n_l \delta_{jk} - \hat{\nu}_{2a}^R \delta_{lx} n_i \delta_{jk} \\
&+\hat{\nu}_{3a}^R \delta_{kx} n_l \delta_{ij} + \hat{\nu}_{3b}^R \delta_{lx} n_k \delta_{ij} - \hat{\nu}_{3b}^R \delta_{ix} n_j \delta_{kl} - \hat{\nu}_{3a}^R \delta_{jx} n_i \delta_{kl}) \\
&+\nu_5^R H\left(\varepsilon_{ikz} n_j n_l + \varepsilon_{ilz} n_j n_k + \varepsilon_{jlz} n_i n_k + \varepsilon_{jkz} n_i n_l\right) \\
&+\nu_7^R H\left(\varepsilon_{ikz}\delta_{jl} + \varepsilon_{ilz}\delta_{jk} + \varepsilon_{jlz}\delta_{ik} + \varepsilon_{jkz}\delta_{il}\right) \\
&+H\left(\hat{\nu}_{8a}^R \varepsilon_{iky}\left(\delta_{jz} n_l + \delta_{lz} n_j\right) + \hat{\nu}_{8b}^R \varepsilon_{ily}\left(\delta_{jz} n_k + \delta_{kz} n_j\right)\right. \\
&\left.+\hat{\nu}_{8c}^R \varepsilon_{jly}(\delta_{iz} n_k + \delta_{kz} n_i) + \hat{\nu}_{8d}^R \varepsilon_{jky}(\delta_{iz} n_l + \delta_{lz} n_i)\right)
\end{aligned} \tag{A.2}$$

with the abbreviations

$$\begin{aligned}
\hat{\nu}_{1a}^R &= \nu_1^R - \frac{\gamma_1}{4}\left((2\lambda_1^D - \lambda_5^D + \lambda_6^D)(\lambda + 1) - 2\lambda_2^D \lambda\right) \\
\hat{\nu}_{1b}^R &= \nu_1^R - \frac{\gamma_1}{4}\left((2\lambda_1^D - \lambda_5^D + \lambda_6^D)(\lambda - 1) - 2\lambda_2^D \lambda\right) \\
\hat{\nu}_{2a}^R &= \nu_2^R - \frac{\gamma_1}{4}(\lambda - 1)\lambda_2^D \\
\hat{\nu}_{2b}^R &= \nu_2^R - \frac{\gamma_1}{4}(\lambda + 1)\lambda_2^D \\
\hat{\nu}_{3a}^R &= \nu_3^R + \frac{\gamma_1}{4}(\lambda - 1)\lambda_6^D \\
\hat{\nu}_{3b}^R &= \nu_3^R + \frac{\gamma_1}{4}(\lambda + 1)\lambda_6^D \\
\hat{\nu}_{8a}^R &= \nu_8^R + \frac{\gamma_1}{4}2\lambda_3^D \\
\hat{\nu}_{8b}^R &= \nu_8^R + \frac{\gamma_1}{4}(\lambda + 1)\lambda_3^D \\
\hat{\nu}_{8c}^R &= \hat{\nu}_{8a}^R \\
\hat{\nu}_{8d}^R &= \nu_8^R + \frac{\gamma_1}{4}(\lambda - 1)\lambda_3^D
\end{aligned} \tag{A.3}$$

Appendix A.3. The linear stability problem in the case when $\boldsymbol{n} \perp \boldsymbol{H}$

In this appendix we present the explicit form of the linear stability problem for the case when $\boldsymbol{n} \perp \boldsymbol{H}$. It can be expressed in the form (29):

$$\begin{aligned}
&-\left(\left(\frac{\gamma_1}{4}(\lambda - 1)^2 + \nu_3\right)k_x^2 + \nu_2 k_y^2\right) f^{IV} \\
&+\left(2\nu_2 + 2\nu_3 + \frac{\gamma_1}{2}\left(1 + \lambda^2\right)\right)k_x^2 k_y^2\, f'' \\
&+\left(\left(2\nu_1 + 2\nu_2 - 3\nu_3 - \frac{\gamma_1}{2}\left(\lambda^2 - 1\right)\right)k_x^4 + 2\nu_2 k_y^4\right) f'' \\
&-\left(\left(\frac{\gamma_1}{4}(1 + \lambda)^2 + \nu_3\right)k_x^6 + \nu_2 k_y^6\right) f \\
&-\left(\frac{\gamma_1}{2}(1 + \lambda)^2 + \nu_2 + 2\nu_3\right)k_x^4 k_y^2\, f \\
&-\left(\frac{\gamma_1}{4}(1 + \lambda)^2 + 2\nu_2 + \nu_3\right)k_x^2 k_y^4\, f \\
&+\left(\frac{\gamma_1}{4}(\lambda - 1)^2 - \nu_2 + \nu_3\right)k_x k_y\, g''' \\
&-\left(\frac{\gamma_1}{4}\left(1 - 2\lambda - 3\lambda^2\right) + 2\nu_1 + \nu_2 - 3\nu_3\right)k_x^3 k_y\, g' \\
&-\left(\frac{\gamma_1}{4}(\lambda - 1)^2 - \nu_2 + \nu_3\right)k_x k_y^3\, g' \\
&+ik_y\left(k_x^2 + k_y^2\right)\left(\left(\overline{H}_2 k_x^2 + \overline{H}_1 k_y^2\right)g - \overline{H}_1\, g''\right) \\
&+(k_x^2 + k_y^2)\mathrm{g}\alpha_p\,\theta \\
&= i\omega\left(k_x^2 + k_y^2\right)\left(k_x^2 + k_y^2 - \frac{d^2}{dz^2}\right)f
\end{aligned} \tag{A.4}$$

$$\begin{aligned}
&-\left(\frac{\gamma_1}{4}(\lambda - 1)^2 - \nu_2 + \nu_3\right)k_x k_y\, f''' \\
&+\left(\frac{\gamma_1}{4}(\lambda - 1)^2 - \nu_2 + \nu_3\right)k_y^2\, f' \\
&-\left(\frac{\gamma_1}{4}(3\lambda - 1)(1 + \lambda) - \nu_1 - \nu_2 + 3\nu_3\right)k_x k_y\, f' \\
&+\left(\left(\frac{\gamma_1}{4}(\lambda - 1)^2 + \nu_3\right)k_y^2 + \nu_2 k_x\right)g'' \\
&-\left(\frac{\gamma_1}{4}\left(k_y^2(\lambda - 1) + k_x^2(1 + \lambda)\right)^2\right)g \\
&-\left(k_x^2 k_y^2\left(2\nu_1 + 2\nu_2\right) - \nu_3\left(k_x^2 - k_y^2\right)^2\right)g \\
&+ik_y(k_x^2 + k_y^2)\left(\left(\overline{H}_2 k_y^2 + \overline{H}_1 k_x^2\right)f - \overline{H}_1\, f''\right) \\
&= i\omega\left(k_x^2 + k_y^2\right)g
\end{aligned} \tag{A.5}$$

$$\begin{aligned}
&\kappa_\perp\theta'' - \left(\kappa_\perp k_y^2 + \left(\kappa_\parallel + \kappa_\perp\right)k_x^2\right)\theta + \frac{T_0 - T_1}{h}(k_x^2 + k_y^2)f \\
&= i\omega\theta
\end{aligned} \tag{A.6}$$

Acknowledgements

Support through SPP1104 'Colloidal Magnetic Fluids' of the Deutsche Forschungsgemeinschaft is gratefully acknowledged.

References

1. F. Brochard and P.G. de Gennes, *J. Phys. (France)* **31** (1970) 691.
2. J. Rault, P.E. Cladis, and J.P. Burger, *Phys. Lett.* **A 32** (1970) 199.
3. C.F. Hayes, *Mol. Cryst. Liq. Cryst.* **36** (1976) 245.
4. L. Liébert and A. Martinet, *J. Phys. Lett.(France)* **40** (1979) 363.
5. S.-H. Chen and S.H. Chiang, *Mol. Cryst. Liq. Cryst.* **144** (1987) 359.
6. J.C. Bacri and A.M. Figueiredo Neto, *Phys. Rev.* **E 50** (1994) 3860.
7. S.I. Burylov and Y.L. Raikher, *Mol. Cryst. Liq. Cryst.* **258** (1995) 123.
8. M. Koneracká, V. Závišová, P. Kopčanský, J. Jadżyn, G. Czechowski, and B. Żywucki, *J. Magn. Magn. Mater.* **157/158** (1996) 589.
9. S. Fontanini, A.L. Alexe-Ionescu, G. Barbero, and A.M. Figueiredo Neto, *J. Chem. Phys.* **106** (1997) 6187.
10. V. Berejnov, J.-C. Bacri, V. Cabuil, R. Perzynski, and Y.L. Raikher, *Europhys. Lett.* **41** (1998) 507.
11. A.Yu. Zubarev and L.Yu. Iskakova, *J. Magn. Magn. Mater.* **183** (1998) 201.
12. Y.L. Raikher and V.I. Stepanov, *J. Magn. Magn. Mater.* **201** (1999) 182 .
13. I. Potočová, M. Koneracká, P. Kopčanský, M. Timko, L. Tomčo, J. Jadżyn, and G. Czechowski, *J. Magn. Magn. Mater.* **196** (1999) 578.
14. C.Y. Matuo and A.M. Figueiredo Neto, *Phys. Rev.* **E 60** (1999) 1815.
15. E. Jarkova, H. Pleiner, H.-W. Müller, A. Fink, and H.R. Brand, *Eur. Phys. J.* **E5** (2001) 583.
16. L.D. Landau, E.M. Lifshitz, and L.P. Pitaevskii, *Electrodynamics of Continuous Media*, 2nd ed., Butterworth-Heinemann (1984).
17. S.H. Chen and N.M. Amer, *Phys. Rev. Lett.* **51** (1983) 2298.
18. S.V. Burylov and Y.L. Raikher, *Mol. Cryst. Liq. Cryst.* **258** (1995) 107.
19. E. Jarkova, H. Pleiner, H.-W. Müller, and H.R. Brand, *J. Chem. Phys.* **118** (2003) 2422.
20. H. Pleiner, E. Jarkova, H.-W. Müller, and H.R. Brand, *Magnetohydrodynamics* **37** (2001) 254.
21. S. Chandrasekhar, *Hydrodynamic and Hydromagnetic Stability*, Clarendon Press, Oxford 1961.
22. H. Pleiner and H.R. Brand, Hydrodynamics and Electrodynamics of Liquid Crystals in *Pattern Formation in Liquid Crystals*, Springer, New York 1996.
23. L. I. Berg, G. Ahlers, and D. Cannell, *Phys. Rev.* **E48** N5 (1993) R3236.
24. D. Forster, T.C. Lubensky, P.C. Martin, J.Swift, and P.S. Pershan, *Phys. Rev. Lett.* **26** (1971) 1016.
25. P.C. Martin, O. Parodi, and P.S. Pershan, *Phys. Rev.* **A6** (1972) 2401.
26. P.G. de Gennes and J. Prost, *The Physics of Liquid Crystals* Clarendon Press, Oxford 1993.
27. N. Li, J.O. Murphy, and J.M. Steiner, *Z. Angew. Math. Mech.* **75** (1995) 3.
28. G. Küppers and D. Lortz, *J. Fluid Mech.* **35** (1969) 609.
29. A.B. Ryskin, H.-W. Müller, and H. Pleiner, *Phys. Rev.* **E67** (2003) 046302.
30. Q. Feng, W. Pesch, and L. Kramer, *Phys. Rev.* **A45** (1992) 45.
31. F.G. Busse, *J. Fluid Mech.* **52** (1972) 97.
32. A. Buka, Viscous Fingering in *Pattern Formation in Liquid Crystals*, Springer, New York 1996 and references therein.
33. P. G. Saffman and G. I. Taylor, *Proc. Roy. Soc. London, Ser.A* **245** (1958) 312.
34. C. Park and G. M. Homsy, *J. Fluid Mech.* **139** (1984) 291.
35. L. Paterson, *J. Fluid Mech.* **113** (1981) 513.